Journal of Engineering Physics and Thermophysics, Vol. 71, No. 6, 1998

3D MODELING OF THERMAL ANNEALING OF ION-IMPLANTED IMPURITIES

M. V. Kazitov, V. V. Nelaev, and
E. F. Nogotov

UDC 621.382

Three-dimensional (3D) mathematical modeling of the technological operations reflects most realistically the physical processes that occur in formation of structural elements of superlarge integrated circuits (SLICs). However multidimensional modeling of the technology of SLIC manufacture requires the use of economical algorithms for numerical solution of the initial mathematical problem. An efficient procedure for calculating numerically the 3D profile of the dopant distribution formed as a result of thermal annealing after implantation is proposed. The problem of the modeling of the diffusional redistribution of the dopant in annealing in an active medium is considered. Some results of calculations are discussed.

Modeling of the Profile of Implants. The basic technological operations of microelectronics are ion implantation, thermal annealing, and surface modification (oxidation, etching, and deposition). As a result of each a new impurity distribution is formed, on which the electrical characteristics of the device depend.

Ion implantation is one of the basic methods of local doping of semiconductor structures. This technological operation is used not only to introduce dopants in semiconductors but also to synthesize new compounds and to alter the mechanical, corrosion, catalytic, and optical properties of surface layers of materials. The improvement of technologies that use ion implantation as a method of controlled introduction of impurities in solids requires an increasingly more accurate description of the distribution of impurity atoms. This is particularly topical when high-energy and high-intensity implantations, short and pulsed annealings, and maskless technologies are used. At present, the problem of an adequate theoretical description of multidimensional profiles of the implant distribution (in cases where orientation effects can be disregarded) has been well studied [1-3]. There are three mutually complementary methods for calculating implant distributions: the method of moments, direct solution of the equations of particle transport in energy-angle space, and modeling of ion trajectories by the Monte Carlo method. The method of moments is optimum in modeling the process of implantation for ion-target pairs with known moments of the statistical distribution.

The postimplantation spatial distribution of the impurity $F(x, y, z)$ is modeled using the integral of the statistical distribution function over the variables η and ξ

$$F(x, y, z) = \frac{1}{4ab} \int_{-a}^{a} \int_{-b}^{b} F^0 (x, y - \eta, z - \xi) \, d\eta d\xi \,, \tag{1}$$

where

$$F^0 (x, y, z) = P (x) \, G (y, \sigma (x)) \, G (z, \sigma (x)) \, .$$

Here $G(y, \sigma(x))$ and $G(z, \sigma(x))$ are Gauss distribution functions with variance varying over the depth:

$$G (y, \sigma (x)) = \frac{Q}{\sigma (x) \sqrt{2\pi}} \exp \left(- \frac{y^2}{2\sigma^2 (x)} \right) . \tag{2}$$

Belarusian State University of Informatics and Radio Electronics. Academic Scientific Complex "A. V. Luikov Institute of Heat and Mass Transfer of the National Academy of Sciences of Belarus," Minsk, Belarus. Translated from Inzhenerno-Fizicheskii Zhurnal, Vol. 71, No. 6, pp. 1075-1080, November-December, 1998. Original article submitted July 11, 1997.

1062-0125/98/7106-1039$20.00 ©1999 Kluwer Academic/Plenum Publishers

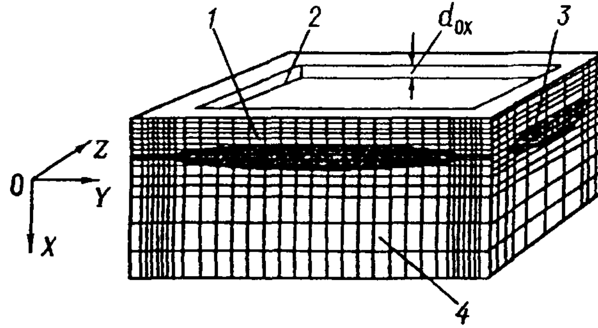

Fig. 1. Coordinate system used in numerical solution of the nonlinear diffusion equation: 1) fictitious region; 2) mask window; 3) oxide; 4) substrate. d_{ox}, oxide width.

The variance of the distribution $\sigma(x)$ is determined by the formula

$$\sigma^2(x) = \Delta Y^2\,[\mathrm{Sk}_y (x - R_p)/\Delta R_p + 1]\,. \tag{3}$$

The Pearson-IV distribution function $P(x)$ is written in the following form [3]:

$$P(X) = K\left[1 + \left(\frac{x'}{\alpha}\right)^2\right]^{-q} \exp\left(-\nu \arctan\frac{x'}{\alpha}\right); \tag{4}$$

$$x' = x - R_p - \left(\alpha\,\frac{\nu}{2\,(q-1)}\right).$$

The parameters α, q, and ν are determined by the first moments of the statistical distribution function:

$$\alpha = \Delta R_p\,[(r-1) - \beta_1 (r-2)^2/16]^{1/2}\,,\quad q = (r+2)/2\,,$$

$$\beta_2 = \beta_1 - \frac{c_1 + c_1^2 + c_2(\beta_1 - 32)}{\beta_1 - 32}\,,\quad c_1 = 39\beta_1 + 48\,,\quad c_2 = 9\beta_1(4\beta_1 + 7)\,, \tag{5}$$

$$\nu = \frac{\mathrm{Sk}\,(r-2)\,r}{[16\,(r-1) - \beta_1 (r-2)^2]^{1/2}}\,,\quad r = \frac{6\,(\beta_2 - \beta_1 - 1)}{(2\beta_2 - 3\beta_1 - 6)}\,,\quad \beta_1 = \mathrm{Sk}^2\,.$$

The variance of the distribution in the transverse direction must be positive, and therefore we need to satisfy the conditions

$$x < R_p + \Delta R_p/|\mathrm{Sk}_y|\,,\quad \mathrm{Sk}_y < 0\,,\quad x > R_p - \Delta R_p/|\mathrm{Sk}_y|\,,\quad \mathrm{Sk}_y > 0\,. \tag{6}$$

Inequalities (6) restrict the applicability of the model in the case of implantation of very slow heavy ions ($E < 1$ keV) when $x \ll R_p$ as well as for light ions at large depths where the function $P(x)$ takes on low values. This enables us to assume $F(x, y, z) = 0$ in the region where inequalities (6) are not satisfied.

Modeling of the Impurity Redistribution in the Process of Postimplantation Thermal Annealing. The diffusional redistribution of impurities in the further postimplantation technological operations of the formation of semiconductor structures is the most important part of the problem of modeling and optimization of the technological operations of microelectronics.

In the general case, the impurity redistribution in thermal annealing is described by the nonlinear diffusion equation

$$\frac{\partial C}{\partial t} = \frac{\partial}{\partial x}\left(D(C)\frac{\partial C}{\partial x}\right) + \frac{\partial}{\partial y}\left(D(C)\frac{\partial C}{\partial y}\right) + \frac{\partial}{\partial z}\left(D(C)\frac{\partial C}{\partial z}\right). \tag{7}$$

At the initial instant $t = 0$, $C(x, y, z) = F(x, y, z)$.

The nonlinearity of Eq. (7) is due to the substantial dependence of the diffusion coefficient D on the concentration C. Figure 1 shows the coordinate system used in 3D modeling of the diffusion impurity distribution and the characteristic points of the spatial grid. The origin of coordinates is on the surface at the center of the window, and the X coordinate is directed into the specimen perpendicular to the surface of the region modeled.

Equation (7) is solved numerically by the finite-difference method and not by the finite-element method traditionally used [5-7]. For convenience and greater clarity of the procedure for synthesizing the numerical algorithm, it is appropriate to represent it in operator form:

$$\frac{\partial C}{\partial t} = L_x C + L_y C + L_z C, \tag{8}$$

where

$$L_x C = \frac{\partial}{\partial x}\left(D(C)\frac{\partial C}{\partial x}\right), \quad L_y C = \frac{\partial}{\partial y}\left(D(C)\frac{\partial C}{\partial y}\right), \quad L_z C = \frac{\partial}{\partial z}\left(D(C)\frac{\partial C}{\partial z}\right).$$

The differential operators are approximated by finite-difference relations of the form

$$L_x C \approx \frac{2}{\Delta x_{k-1} + \Delta x_k}\left[\frac{D_{k+1/2,l,m}}{\Delta x_k}(C_{k+1,l,m} - C_{k,l,m}) - \frac{D_{k-1/2,l,m}}{\Delta x_{k-1}}(C_{k,l,m} - C_{k-1,l,m})\right], \tag{9}$$

Then, for

$$Dx_{k\pm 1/2,l,m} = D\left(\frac{x_{k\pm 1} + x_k}{2},\ y_l,\ z_m\right), \quad Hx_k = \frac{2}{\Delta x_{k-1} + \Delta x_k},$$

$$Dx_k = \frac{D_{k-1/2,l,m}}{\Delta x_{k-1}}, \quad Dx_{k+1} = \frac{D_{k+1/2,l,m}}{\Delta x_k}.$$

$$L_x C \approx Hx_k\,[Dx_{k+1}(C_{k+1,l,m} - C_{k,l,m}) - Dx_k(C_{k,l,m} - C_{k-1,l,m})].$$

We approximate the differential operators $L_y C$ and $L_z C$ similarly.

To solve the diffusion equation (7), we used the "predictor-corrector" method [4]. In the predictor step, the concentrations of the impurities $C(x, y, z)$ at the grid nodes are calculated by an implicit scheme without allowance for the flow as a function of the spatial directions (X, Y, Z). In the corrector step, the concentrations at the nodes of the grid are calculated by an explicit scheme based on the results obtained in the predictor step. The system of equations of the predictor

$$C^1_{k,l,m} - C^n_{k,l,m} = 0.5\,\Delta t\,L_x C^1_{k,l,m}, \quad C^2_{k,l,m} - C^1_{k,l,m} = 0.5\,\Delta t\,L_y C^2_{k,l,m},$$
$$C^3_{k,l,m} - C^2_{k,l,m} = 0.5\,\Delta t\,L_z C^3_{k,l,m} \tag{10}$$

was solved by the method of running. Next, by the explicit scheme

$$C^{n+1}_{k,l,m} = C^n_{k,l,m} + \Delta t\,(L_x C^3_{k,l,m} + L_y C^3_{k,l,m} + L_z C^3_{k,l,m}) \tag{11}$$

we corrected the results obtained. On each time interval, we refined the diffusion coefficients iteratively.

For calculation of the diffusion coefficient D, as in the SUPREM program for the modeling of technological processes in microelectronics [5, 6], use was made of the vacancy model

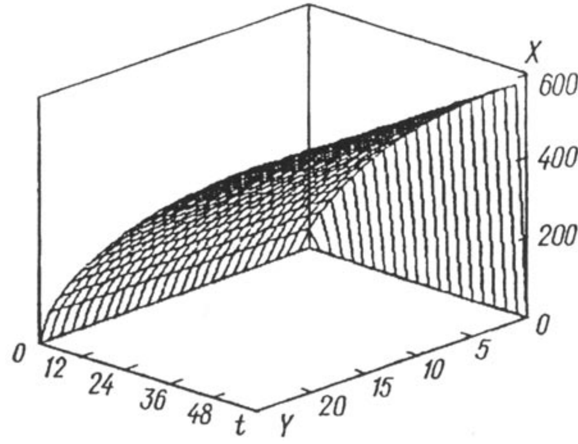

Fig. 2. Result of two-dimensional modeling of oxide growth (X_0 = 10 Å; γ = 1; $B = 3.92 \cdot 10^4$ Å^2/min; $B/A = 46.3$ Å/min; $T = 1100$ °C; the partial pressure of the oxygen is $P_{O_2} = 10^5$ Pa). t, min; X and Y, Å.

$$D = h \left[D^0 + D^+ \left(\frac{p}{n_i} \right) + D^- \left(\frac{n}{n_i} \right) + D^= \left(\frac{n}{n_i} \right)^2 \right],$$

where

$$n_i = \left[1.5 \cdot 10^{33} T^3 \exp \left(- \frac{1.21 \text{ eV}}{kT} \right) \right]^{1/2} \text{ cm}^{-3}, \quad D^\nu = D_0 \exp \left(- \frac{E_a}{kT} \right). \tag{12}$$

The diffusion acceleration factor h is determined by the formula

$$h = 1 + ZN \frac{\partial \ln (N/n_i)}{\partial N}, \tag{13}$$

and the indices ν = 0, +, −, = refer, respectively, to the neutrally, positively, negatively, and doubly negatively charged impurity.

The introduction of a fictitious region above the substrate enabled us to model the impurity redistribution for the substrate and oxide regions by a unified numerical scheme. Differences between the oxide and the substrate were allowed for in calculating the diffusion coefficient. This approach requires an increase in the number of grid nodes; however, here the computational algorithm is simplified substantially since the need for reconstructing the spatial grid in each time step disappears.

The discontinuous diffusion coefficient makes the requirements on the size of the time and space steps of the grid more rigorous, which leads to the necessity of introducing a variable space step. In constructing a spatial grid with a variable step, the condition $0.7 \le h_k/h_{k+1} \le 1.3$ was obeyed. Numerical experiments showed that violation of this condition, as a rule, leads to deteriorated convergence and accuracy of the results obtained.

The problem was solved in the rectangular region $\Omega = \{0 \le x \le X;\ 0 \le y \le Y;\ 0 \le z \le Z\}$, where X, Y, and Z were chosen such that the concentration $C(x, y, z)$ at the boundaries practically did not change. The region Ω involved fictitious nodes at which C was assumed to be zero. At the boundary of the region, we prescribed the symmetry condition $\partial C/\partial n = 0$ (n is the external normal). The size of the fictitious region (see Fig. 1) was chosen on the basis of the assumed oxide thickness, which can be estimated quite accurately from the empirical dependences [7] (see Fig. 2)

$$X_{SiO_2}(y, t) = X(t) \frac{1}{2} \left[1 + \text{erf} \left(\frac{\sqrt{2}}{\gamma} \frac{y}{X(t)} \right) \right], \tag{14}$$

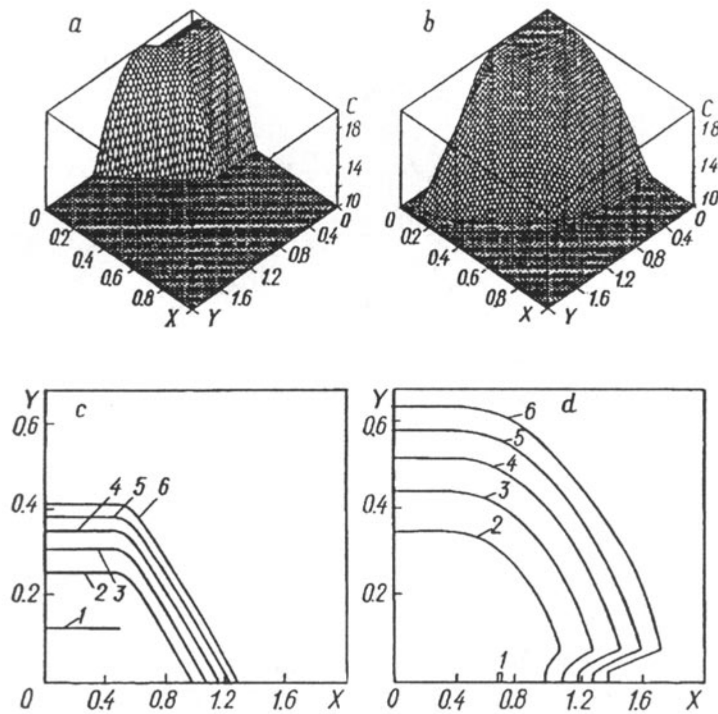

Fig. 3. Results of a three-dimensional calculation of the phosphorus profile in a silicon substrate as a result of implantation (a and b) and numerical modeling of annealing in an oxidizing medium (c and d): a and b) calculated profiles in the cross section $z = 0$; c and d) isoconcentration lines of the calculated profiles; c: 1) $C = 8.4 \cdot 10^{19}$ cm^{-3}; 2) $1.9 \cdot 10^{18}$; 3) $4.1 \cdot 10^{16}$; 4) $9.2 \cdot 10^{14}$; 5) $2.0 \cdot 10^{13}$; 6) $4.5 \cdot 10^{11}$; d: 1) $C = 6.51 \cdot 10^{19}$ cm^{-3}; 2) $1.5 \cdot 10^{18}$; 3) $3.5 \cdot 10^{16}$; 4) $8.1 \cdot 10^{14}$; 5) $1.9 \cdot 10^{13}$; 6) $4.3 \cdot 10^{11}$. C, cm^{-3}; X and Y, μm.

$$X(t) = -\frac{A}{2} + \sqrt{\left(\left[\frac{A^2}{4} + B(t + t_0)\right]\right)}, \qquad (15)$$

$$t_0 = \frac{1}{B}(X_0^2 + AX_0).$$

Calculations showed that the process of impurity redistribution is nonuniform in time. At first it proceeds more rapidly as a rule, but then it is retarded. In this connection, it is appropriate to introduce a variable time step. Depending on the number of iterations in the previous time step, the time step is altered by the procedure described in [8].

This approach enables us to improve significantly the adaptivity of the method since the allowable size of the time step Δt depends substantially on such parameters as the type of impurity, the annealing temperature, the implantation dose, etc.

Software Impementation. The given numerical scheme was implemented in a C language (the ANSI standard), which solves the problem of transferring the mathematical part of the program to different hardware platforms. The program was tested on two platforms: UNIX (SUN 50 MHz) and Windows 95 (Pentium 120 MHz/16 Mb). Calculations showed that the rate of modeling was approximately the same on both platforms. This result is confirmed by the fact that modern Pentium/Pentium Pro personal computers came quite close to inexpensive workstations in performance. Since the Windows NT operating system is universal in relation to hardware platforms, in developing software applications, it makes sense to orient oneself to a Windows operating system. The interface part is realized using a Delphi visual-programming system, which permits, on the one hand, use of the mathematical part of the program in projects developed for UNIX, MacOS, etc. and, on the other, elimination of

routine work on producing the interface part and the engineering database needed to solve a problem of statistical modeling.

Figure 3 gives results of modeling the redistribution of ion-implanted phosphorus in a silicon substrate as a result of thermal annealing. The parameters of the implantation are: the implanted-ion energy $E = 100$ keV; the dose $Q = 10^{15}$ cm^{-2}, and the mask dimensions 1×1 μm. The parameters of the annealing are: the temperature $T = 1020^{\circ}$C, the time $t = 60$ min, a medium of dry oxygen. The computational grid had the dimensions $50 \times 50 \times 50$. The results of the modeling are given for the cross section $z = 0$.

The calculation of 120 time steps of modeling phosphorus diffusion in silicon on a Pentium 120 personal computer took about 15 min.

The chosen model and the developed numerical algorithm make it possible to quite efficiently perform 3D modeling of the redistribution of an ion-implanted impurity in the process of thermal annealing in active and passive media. At a later time it is planned to use the program developed for straight-through statistical modeling of the process of forming SLIC elements. It is hoped that, in the near future, straight-through multidimensional design of the process of SLIC production on ordinary personal computers will be made possible.

NOTATION

Q, implant dose; β_1, asymmetry; β_2, excess; ΔR_p, straggling; R_p, projective path of the ion; Sk_y, combined asymmetry; K, normalizing factor; ΔY, lateral straggling; α, slope of the mask's edge; $C(x, y, z)$, impurity concentration as a function of the coordinates; k, Stefan–Boltzmann constant; Z', charge state of the impurity; D_0^v and E_a^v, parameters that characterize the coefficient of impurity diffusion; γ, fitting parameter, chosen on the basis of the slope of the oxide's edge; $X(t)$, thickness of the one-dimensional oxide, i.e., the oxide produced in the absence of a masking layer; B and B/A, parabolic and linear constants of the rate of oxide growth; X_0, initial thickness of the oxide layer; t, time of the process; T, temperature. Subscripts and superscripts: i, characteristic of the intrinsic semiconductor; k, l, and m, numbers of the nodes of the grid along the x, y, and z directions, respectively; a, activation characteristic; p, projective.

REFERENCES

1. H. Ryssel, K. Haberger, K. Hoffmann, G. Prinke, R. Dümcke, and A. Sachs, IEEE Trans. Electron Devices, ED-27, No. 8, 1484-1490 (1980).
2. S. Furukawa, H. Matsumura, and H. Ishiwara, Jpn. J. Appl. Phys., 11, No. 2, 134-142 (1972).
3. F. F. Komarov, A. N. Novikov, and A. F. Burenkov, Ion Implantation [in Russian], Minsk (1994).
4. B. M. Berkovskii and E. F. Nogotov, Difference Methods for Investigating Problems of Heat Transfer [in Russian], Minsk (1979).
5. C. P. Ho, J. D. Plummer, S. E. Hansen, and R. W. Dutton, IEEE Trans. Electron Devices, ED-30, No. 11, 1438-1452 (1983).
6. M. E. Law and R. W. Dutton, IEEE Trans. Computer-Aided Design, CAD-7, No. 2, 181-189 (1988).
7. R. Penumalli, Proc. 2nd Int. Conf. on Numerical Analysis of Semiconductor Devices and IC's (NASECODE II), Dublin, Ireland (1981), pp. 212-215.
8. M. V. Kazitov, V. V. Nelaev, and E. F. Nogotov, Vestnik Svyazi, No. 2, 44 (1996).